Thin Solid Films 597 (2015) 183–187

Contents lists available at ScienceDirect

Thin Solid Films

journal homepage: www.elsevier.com/locate/tsf

Indium doped $Cd_{1-x}Zn_xO$ alloys as wide window transparent conductors

Wei Zhu [a,b], Kin Man Yu [a,c,*], W. Walukiewicz [a]

[a] Materials Sciences Division, Lawrence Berkeley National Laboratory, Berkeley, California 94720, United States
[b] Department of Physics, The Center for Physical Experiments, University of Science and Technology of China, Hefei, Anhui 230026, PR China
[c] Department of Physics and Materials Science, City University of Hong Kong, Kowloon, Hong Kong

ARTICLE INFO

Article history:
Received 7 July 2015
Received in revised form 27 October 2015
Accepted 18 November 2015
Available online xxxx

Keywords:
Transparent conducting oxides
Cadmium oxide
Zinc oxides
Full spectrum photovoltaics

ABSTRACT

We have synthesized Indium doped $Cd_{1-x}Zn_xO$ alloys across the full composition range using magnetron sputtering method. The crystallographic structure of these alloys changes from rocksalt (RS) to wurtzite (WZ) when the Zn content is higher than 30%. The rocksalt phase alloys in the composition range $0 < x < 0.3$ can be efficiently n-type doped, shifting the absorption edge to 3.25 eV and reducing resistivity to about 2.0×10^{-4} Ω-cm. We found that In doped CdO (ICO) transmits more solar photons than commercial fluorine doped tin oxide (FTO) with comparable sheet conductivity. The infrared transmittance is further extended to longer than 1500 nm wavelengths by depositing the In doped $Cd_{1-x}Zn_xO$ in ~1% of O_2. This material has a potential for applications as a transparent conductor for silicon and multi-junction solar cells.

1. Introduction

Transparent conducting oxides (TCOs) are widely used for a variety of applications including photovoltaic solar cells, flat-panel displays, and optoelectronic devices [1–6].Common TCO used today such as Indium Tin Oxide (ITO) or Al doped ZnO (AZO) can have high conductivity (>5000 S/cm) and good transparency over the visible and ultraviolet part of the solar spectrum (300 to 1000 nm). An important drawback of the currently available TCOs is the limited transparency for the long wavelength photons restricting use of these materials for PV (photovoltaic) technologies that do not depend on efficient utilization of the infrared part of the solar spectrum. Consequently the current TCOs cannot be used in two very important technologies, Si PVs and high efficiency multi-junction solar cells. The limitations on the infrared transparency of the TCOs can be attributed to the relatively large plasma frequency and high free carrier absorption.

It has been shown recently that properly doped CdO can have electron concentration exceeding 10^{21} cm^{-3} and mobility higher than any of the previously studied TCOs [7–11]. The large static dielectric constant $\varepsilon_s = 22$ results in efficient screening of ionized impurities giving rise to high mobility of CdO. The reduced ionized impurity scattering leads to reduced free carrier absorption. Also, the large high frequency dielectric constant $\varepsilon_\infty = 5.3$ shifts the plasma reflection edge to longer wavelengths, and thus extending the transmission spectrum to the infra-red [11]. Although the intrinsic gap of CdO is only 2.2 eV, its absorption edge can be increased by the Burstein Moss effect to as high as 3.2 eV for heavily doped materials. However, this is still insufficient to efficiently transmit shorter wavelength UV (ultraviolet) light in the solar spectrum.

Detert al. [12,13] previously showed that the structural mismatch between ZnO and CdO creates two distinct regimes of optical and electrical behavior of $Cd_{1-x}Zn_xO$ alloys. The Zn-rich wurtzite phase alloys exhibit a reduction in the absorption edge energy across the visible spectrum from 3.3 to 1.7 eV with x decreasing from 1 to 0.31. A phase transition to the rocksalt structure at $x = 0.31$ is associated with an abrupt step-like increase in the electron mobility from 20 up to 90 cm^2/Vs and an intrinsic gap from ~1.7 eV to 2.6 eV.

In this work we explore the possibility of improving the UV transparency and the conductivity of rocksalt phase $Cd_{1-x}Zn_xO$ alloys with Indium doping. We found that In doped rocksalt phase $Cd_{1-x}Zn_xO$ with $x \sim 0.2$ can achieve a high electron concentration of 8×10^{20} cm^{-3} with mobility as high as ~60 cm^2/Vs. The absorption edge of these alloys is blue shifted to >3.2 eV without significantly affecting the infrared transmission. Comparing the overall transmission of the solar spectrum of an In doped $Cd_{1-x}Zn_xO$ with a standard TCO (fluorine doped tin oxide (FTO)), we demonstrate that for most thin film PV device applications the In doped $Cd_{1-x}Zn_xO$ transmits more solar photons than a FTO of similar sheet resistance.

2. Experimental

In doped $Cd_{1-x}Zn_xO$ alloys were deposited by radio-frequency (RF) magnetron sputtering using two separate targets: ZnO and CdO doped with nominally 2% In. The composition of the alloys was controlled by varying the power as well as the target-substrate distances of these two targets. Since the In originates from the CdO:In target, we expect

* Corresponding author at: Department of Physics and Materials Science, City University of Hong Kong, Kowloon, Hong Kong.
E-mail address: kinmanyu@cityu.edu.hk (K.M. Yu).

http://dx.doi.org/10.1016/j.tsf.2015.11.052
0040-6090/

the In content in the samples to vary linearly with CdO fraction of the alloy. The films were deposited on soda lime microscope glass slides at 240 °C in either pure argon (Ar) or Ar/O_2 (1% O_2) at a pressure of ~5 mTorr controlled by a mass flow controller and by adjusting the valve between deposition chamber and turbo pump. The composition and thickness of the samples were measured by Rutherford backscattering spectrometry (RBS) using a 3 MeV He^+ ion beam. The thickness of the films ranged from 150 to 200 nm. The crystalline structure of the films was measured by x-ray diffraction (XRD) using a Siemens D500 diffractometer. Electrical properties were determined by Hall Effect measurements in the van der Pauw geometry using an Ecopia HMS3000 system with a 0.6 T magnet. Optical properties of the films were determined from optical transmission and reflection measurements performed at room temperature with a Perkin-Elmer Lambda 950 spectrophotometer.

3. Results and discussion

3.1. Composition and structure

Fig. 1(a) shows X-ray diffraction (XRD) patterns of In doped $Cd_{1-x}Zn_xO$ alloys samples across the full composition range. All films are polycrystalline. The figure can be divided into 3 composition regions: 1) $x < 0.28$, RS region, 2) $x > 0.5$, WZ region, and 3) $0.3 < x < 0.45$, mixed phase region. In the RS single phase region ($x < 0.28$) two diffraction peaks at 2θ ~33–34° and 38–39° are observed corresponding respectively to the (111) and (200) planes of RS $Cd_{1-x}Zn_xO$. Grain size of these films was calculated from the XRD peak width using the Sherrer equation. We found that RS $Cd_{1-x}Zn_xO$ films have grain size ~17 nm and does not vary significantly with composition. WZ $Cd_{1-x}Zn_xO$, on the other hand have grain size varies from 14 to 20 nm when x increases from 0.5 to 1.

In the RS region, a monotonic increase in the diffraction angles for both the (111) and (200) peaks is observed with increasing ZnO content in the alloy films indicating that the lattice parameter is reduced when Cd is substituted with Zn. In contrast, in the WZ phase region with $x > 0.5$ only a single (0002) WZ phase diffraction peak is observed. This suggests that the films exhibit (0001) texture, similar to the structure for ZnO grown by sputtering and pulsed laser deposition on amorphous silicon [5]. This (0002) peak of the WZ phase also shifts to higher angle as x increases, consistent with the decrease in the lattice parameter as more Zn atoms substitute the group II sublattice sites. Both the WZ (0002) and the RS (111) diffraction peaks are observed for the alloy in the composition range of $0.3 < x < 0.45$. Notice that the positions of these peak do not vary but the relative intensity of WZ (0002) peak increases while that of the RS (111) decreases as x increases. This suggests that in the phase transition region, grains of both RS and WZ phases with constant compositions($x \sim 0.3$ for RS and $x \sim 0.5$ for WZ) co-exist and relative fractions of the WZ grains increases and RS grains decrease with increasing ZnO content. This phase change is consistent with results previously reported by Detert et al. on undoped $Cd_{1-x}Zn_xO$ synthesized by pulsed filtered cathodic arc deposition [12].

The observed shifts of diffraction peaks shown in Fig. 1(a) for both the RS and WZ phases are consistent with the reduction of the crystal lattice parameters upon substitution of Cd with Zn in both phases. The amount of substitutional Zn in $Cd_{1-x}Zn_xO$ alloys can be derived from the shift of the diffraction peak using Vegaard's law. Here we use the values of 4.689 Å (5.631 Å) and 4.224 Å (5.194 Å) for the lattice parameters of the RS (WZ) phase of CdO and ZnO, respectively [14,15]. Fig. 1(b) compares the Zn content determined from RBS and XRD. In both RS and WZ regions the Zn content determined by XRD is slightly lower than that obtained from RBS measurements. We note that RBS measures the total Zn concentration whereas the peak shifts in XRD arise from lattice parameter change due to the substitution of Cd with Zn. Therefore the results in Fig. 1(b) suggest that a small fraction of Zn atoms may not be substitutional on cation sites. These non-substitutional atoms can exist in the form of small precipitates of metallic Zn or ZnO at grain boundaries. It should be pointed out that the lattice parameters measured by XRD can also be affected by a stress in the films. Hereafter, we refer to the composition of the films measured by the RBS.

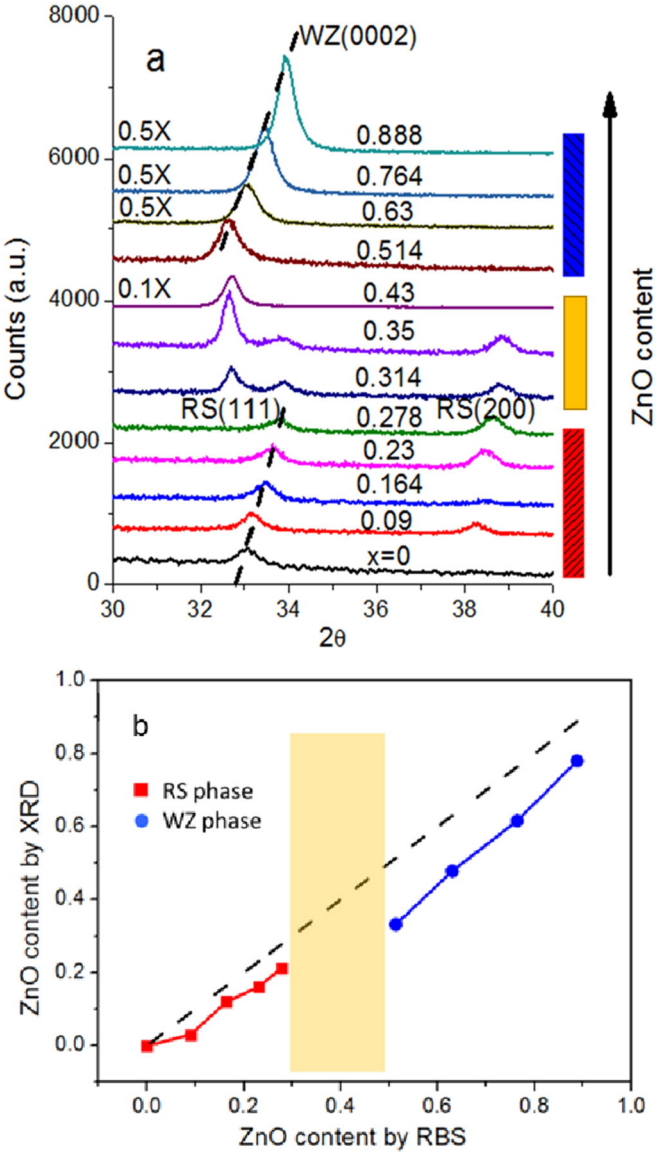

Fig. 1. (a) The XRD results from a series of In doped $Cd_{1-x}Zn_xO$ alloys with x ranging from 0 to 1, and (b) comparison of ZnO content determined by X-Ray diffraction and Rutherford backscattering. Red squares and blue circles represent rocksalt and wurtzite phases, respectively and the shaded region indicates that composition region with mixed RS and WZ phases. (For interpretation of the references to color in this figure legend, the reader is referred to the web version of this article.)

3.2. Electrical properties

The composition dependence of the electron concentration and electron mobility in $Cd_{1-x}Zn_xO$ is shown in Fig. 2. Both the electron concentration and the mobility decrease with increasing Zn content. We note however that since we use a single CdO:In target to change the Cd content and to dope with In, the In concentration should also scale with the Cd content. The reduction in the mobility with increasing Zn content for $Cd_{1-x}Zn_xO$ films shown in Fig. 2 can be attributed to the previously observed reduced mobility in Zn-rich alloys [12] and increasing compensation ratio in low electron concentration sample.

Because of the changes in In doping with composition, instead of comparing the free electron concentration of the films, it may be more

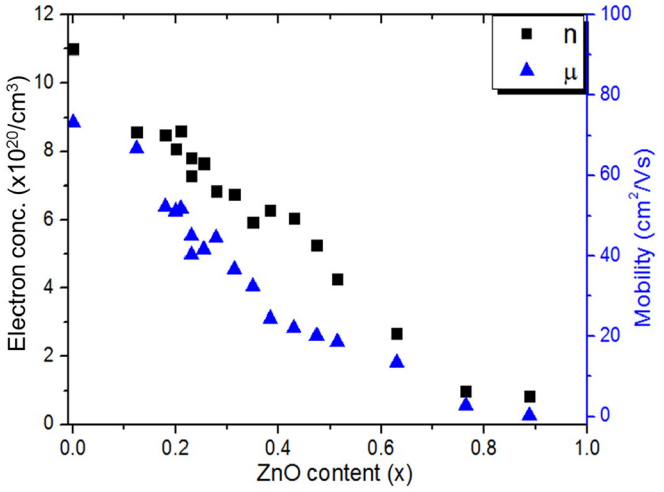

Fig. 2. The electrical property of the In doped $Cd_{1-x}Zn_xO$ alloys.

instructive to look at the change of the In donor activation efficiency, $f_{act}(x)$ in the $Cd_{1-x}Zn_xO$,

$$f_{act}(x) = \frac{n(x)}{[n(0) \times (1-x)]},$$

where $n(x)$ is the electron concentration in In doped $Cd_{1-x}Zn_xO$, $n(0)$ is the electron concentration of CdO:In film. Here we assume that the In content in the CdO:In film is the same as the electron concentration, i.e. $f_{act}(0) = 1$.

The results shown in Fig. 3 indicate that the donor activation efficiency remains almost constant for $0 < x < 0.4$. This reveals that the RS-$Cd_{1-x}Zn_xO$ phase can be doped as efficiently as CdO. For example, for RS $Cd_{1-x}Zn_xO$ with x ~ 0.2, an electron concentration $n = 8 \times 10^{20}$ cm^{-3} with mobility >50 cm^2/Vs can be achieved. This corresponds to a material with resistivity $<1.5 \times 10^{-4}$ Ω-cm, lower than the resistivity of most conventional TCO used today. Notice that the resistivity of this material can be further reduced by optimizing the In doping. A drastic drop in the activation efficiency occurs for alloys with $x > 0.4$, suggesting that $Cd_{1-x}Zn_xO$ in the WZ phase cannot be doped as efficiently with In. Using ion irradiation, x-ray photoelectron spectroscopy as well as soft x-ray absorption and emission measurements, Detert et al. have shown that in the whole WZ phase composition range the conduction band minimum (CBM) of $Cd_{1-x}Zn_xO$

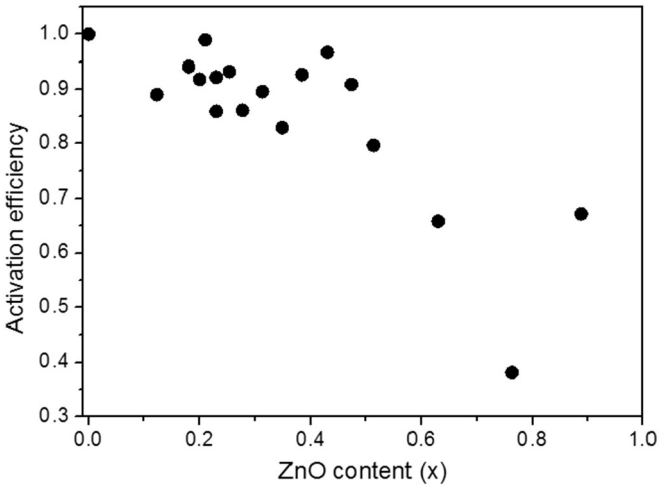

Fig. 3. Activation efficiency of In donor in $Cd_{1-x}Zn_xO$ alloys.

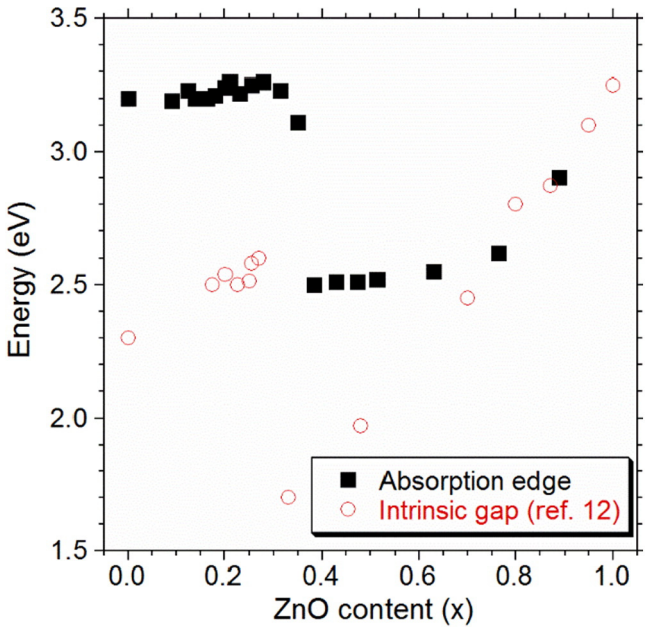

Fig. 4. The optical absorption edge of In doped $Cd_{1-x}Zn_xO$ alloys plotted together with intrinsic band gap taken from Ref. [12].

remained approximately constant relative to the vacuum level [13]. Since the CBM of ZnO is ~0.8 eV higher than that of CdO, a much less efficient n-type doping is expected for the WZ phase $Cd_{1-x}Zn_xO$ alloys. This assertion is consistent with the observed composition dependent donor activation efficiency shown in Fig. 3 [12].

3.3. Optical properties

The composition dependence of the optical absorption edge in In doped $Cd_{1-x}Zn_xO$ alloys is shown in Fig. 4. The composition dependence of the intrinsic gap of $Cd_{1-x}Zn_xO$ alloys has been reported previously by Detert et al. [12] and the values are also included in Fig. 4 for comparison. The intrinsic gap values were obtained by taking into account the carrier induced effects, including the Burstein–Moss shift as well as electron–electron and electron-ion renormalization effects. The observed gradual increase of the absorption edge energy from 3.20 eV in CdO to about 3.25 eV in $Cd_{0.7}Zn_{0.3}O$ is very significant because this upward shift of the absorption edge occurs despite the fact that, as is shown in Fig. 2, the electron concentration decreases from 1.1×10^{21} cm^{-3} in CdO to about 7×10^{20} cm^{-3} in $Cd_{0.7}Zn_{0.3}O$ due to the lowering of In doping as x increases. Considering the amount of the Burstein Moss shift [16] previously observed in CdO we can expect a shift of the absorption edge to about 3.45 eV (360 nm) in $Cd_{0.7}Zn_{0.3}O$ with an electron concentration of ~10^{21} cm^{-3} when the In dopant concentration is further increased. The drastic drop in the absorption edge energy for x ~ 0.3 to 0.4 corresponds to the transition from RS to the WZ phase and is consistent with previous findings that WZ $Cd_{1-x}Zn_xO$ has smaller intrinsic band gap [12].

3.4. Solar photon transmittance

In order to evaluate advantages of CdO based materials compared with standard TCOs we have compared total solar photon fluxes transmitted by a CdO:In (ICO) and a commercial fluorine doped tin oxide (FTO). Note that the absorption edge of the ICO film is 3.2 eV, lower than that of an RS $Cd_{1-x}Zn_xO$:In film. Fig. 5 shows the transmission spectra of a 150 nm thick ICO and a 540 nm thick FTO films with the sheet resistances of 5 Ω/□ and 7 Ω/□, respectively together with the solar photon flux spectrum. The ICO film exhibits a somewhat lower

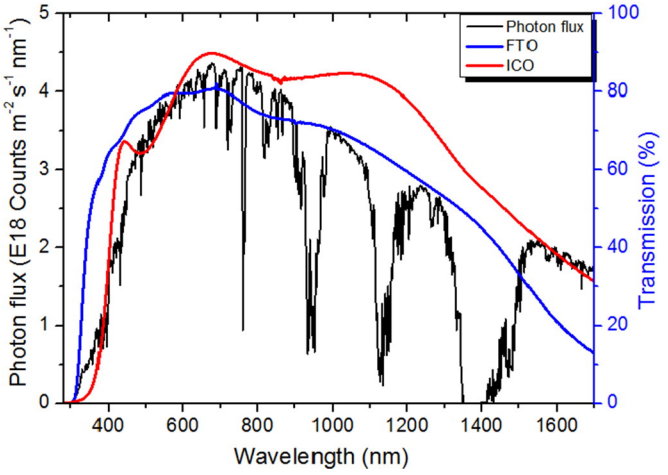

Fig. 5. The Photon flux spectrum of solar spectrum (AM 1.5), and transmission spectra of ICO and FTO thinfilms.

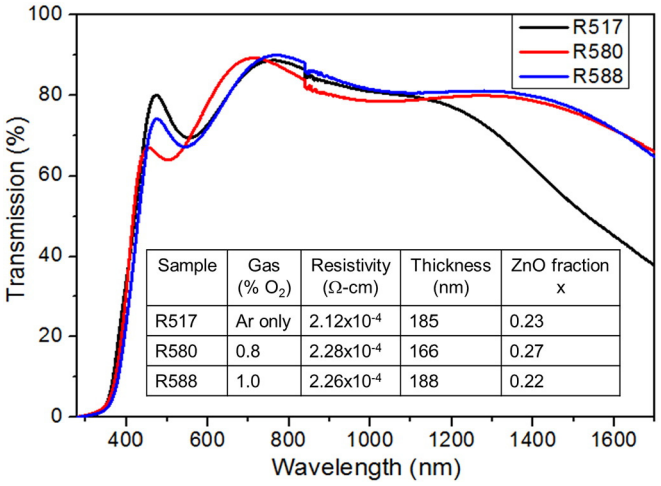

Sample	Gas (% O_2)	Resistivity (Ω-cm)	Thickness (nm)	ZnO fraction x
R517	Ar only	2.12×10^{-4}	185	0.23
R580	0.8	2.28×10^{-4}	166	0.27
R588	1.0	2.26×10^{-4}	188	0.22

Fig. 7. Transmission spectra of the ICOs deposited under different ambient gas.

transmission for the wavelength shorter than 600 nm but a much higher transmission at longer wavelengths. This indicates that ICO would serve as a better TCO for PV absorbers with lower energy gap.

The photon flux spectrum shown in Fig. 5 is obtained by dividing the solar power irradiation spectrum by the photon energy. The solar irradiation spectrum at AM 1.5 has been adopted from www.pveducation.org. Fig. 5 shows the importance of the IR part of the solar spectrum for the performance of PV devices. The fluxes of transmitted photons are obtained by multiplying the total photon flux and the transmission curves for ICO and FTO. Fig. 6 shows the cumulative photon flux as a function of the cutoff wavelength (λ) of a PV absorber obtained by integrating the fluxes of transmitted photons from the short wavelength limit of the solar spectrum to λ.

Fig. 6 reveals that the small disadvantage of ICO (<1%) in the short wavelength region λ < 800 nm due to the smaller bandgap of CdO is compensated by a much higher transmission in the infrared part of the solar spectrum, making ICO a better transparent conductor for the absorbers with the cutoff wavelength longer than about 900 nm. The total flux of the photons transmitted through the transparent contact is especially important for the Si solar cells with the band gap of 1.1 eV (1130 nm). In this case, about 7.5% more solar photons is transmitted through ICO compared with FTO film with similar sheet conductivity.

We have also found that properties of In doped $Cd_{1-x}Zn_xO$ alloys are very sensitive to the deposition conditions, in particular to the sputtering gas composition. Typically adding a small amount of O_2 (~1%) to the Ar sputtering gas reduces the electron concentration by ~20% and increases electron mobility by 10–20%. As a consequence, the infrared transmittance of $Cd_{1-x}Zn_xO$ alloys is improved. Fig. 7 shows the transmission spectra of $Cd_{1-x}Zn_xO$ films with similar resistivity of 2.2×10^{-4} Ω-cm deposited in Ar gas only and with the addition of 0.8 and 1% of O_2. Significant improvement in the IR transmission is observed for films deposited with O_2. This effect can be attributed to change in the film stoichiometry resulting in lower electron concentration but higher mobility and thus also reduced free carrier absorption and increase in the plasma reflection wavelength [11]. However, the films grown with O_2 content larger than 2% in the sputtering gas have significantly lower electron concentration and mobility due to the formation of acceptor type O interstitial and Cd vacancy defects.

In order to compare the advantages of ICOs grown under different conditions with FTO we have calculated total transmitted photon fluxes for the absorbers with the band gap of Si (1.1 eV) and Ge (0.7 eV). The results in Fig. 8 show a clear advantage of using ICO compared with commercial FTO. This improvement is particularly significant for Ge absorbers where the film grown in an ambient gas with 1% O_2 has about 18.2% higher transmitted photonflux than FTO. This offers an interesting possibility of using ICO as a transparent contact for Ge and/or InGaAs based triple-junction solar cells [17].

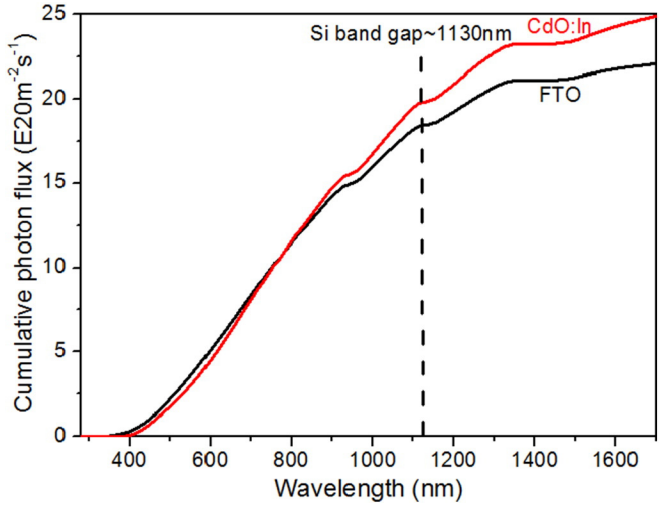

Fig. 6. The cumulative photon flux spectra of ICO and FTO thinfilms.

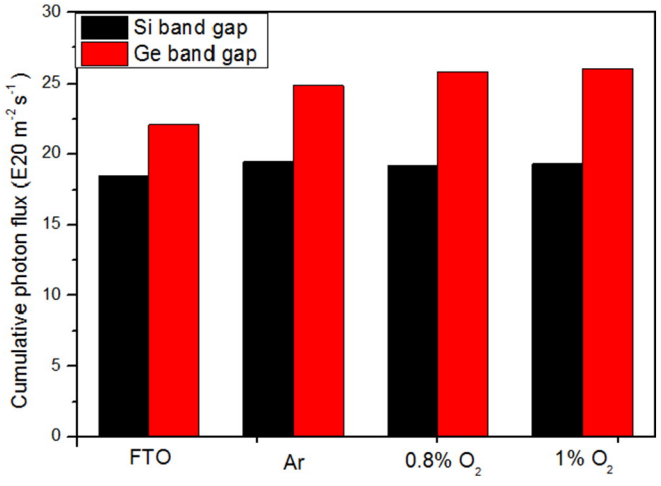

Fig. 8. Cumulative photon flux of FTO and ICOs grown under different conditions.

4. Conclusions

We have synthesized and characterized a series of In doped $Cd_{1-x}Zn_xO$ alloys across the full composition range. The crystallographic structure changes from RS toWZ with increasing Zn content. A mixed phase is observed for the composition range $0.3 < x < 0.45$. The donor activation efficiency is high and remains almost constant for alloys with $0 < x < 0.4$, suggesting that the RS-$Cd_{1-x}Zn_xO$ phase can be doped as efficiently as CdO. In addition, alloying of CdO with less than 30% ZnO results in expansion of the transparency window with the absorption edge shifted to 3.25 eV and the IR transmission extended to wavelengths longer than 1500 nm. Comparison of the total transmitted solar photon fluxes demonstrates an advantage of In doped $Cd_{1-x}Zn_xO$ alloys over commercially available FTO for most PV technologies. Finally our results show that adding Oxygen to the sputtering gas has a strong effect on electrical and optical properties of In doped $Cd_{1-x}Zn_xO$ alloy films. This effect can be used to further improve and optimize properties of the CdO based films as transparent conductors for different photovoltaic technologies.

Acknowledgments

This work was supported by the Department of Energy through the Bay Area Photovoltaic Consortium under Award Number DE-EE0004946. Wei Zhu acknowledges support from the Oversea Academic Training Funds of USTC.

References

[1] K. Ellmer, Past achievements and future challenges in the development of optically transparent electrodes, Nat. Photonics 6 (2012) 809–817.
[2] P.D.C. King, T.D. Veal, Conductivity in transparent oxide semiconductors, J. Phys. Condens. Matter 23 (2011) 334214.
[3] M.W. Rowell, D. Michael, McGehee, transparent electrode requirements for thin film solar cell modules, Energy Environ. Sci. 4 (2011) 131–134.
[4] D.S. Ginley, H. Hosono, D.C. Paine (Eds.), Handbook of Transparent Conductors, Springer, New York, 2011.
[5] K. Ellmer, A. Klein, B. Rech (Eds.), Transparent Conductive Zinc Oxide: Basics and Applications in Thin Film Solar Cells (Springer Series in Materials Science, vol. 104, Springer, New York, 2008.
[6] C.G. Granqvist, Transparent conductors as solar energy materials: a panoramic review, Sol. Energy Mater. Sol. Cells 91 (2007) 1529–1598.
[7] M. Yan, M. Lane, C.R. Kannewurf, R.P.H. Chang, Highly conductive epitaxial CdO thin films prepared by pulsed laser deposition, Appl. Phys. Lett. 78 (2001) 2342–2344.
[8] A. Wang, J.R. Babcock, N.L. Edleman, A.W. Metz, M.A. Lane, R. Asahi, V.P. Dravid, C.R. Kannewurf, A.J. Freeman, T.J. Marks, Indium–cadmium–oxide films having exceptional electrical conductivity and optical transparency: clues for optimizing transparent conductors, Proc. Natl. Acad. Sci. 98 (2001) 7113–7116.
[9] B.J. Zheng, J.S. Lian, L. Zhao, Q. Jiang, Optical and electrical properties of In-doped CdO thin films fabricated by pulse laser deposition, Appl. Surf. Sci. 256 (2010) 2910–2914.
[10] Y. Yu, S. Jin, J.E. Medvedeva, J.R. Ireland, A.W. Metz, J. Ni, M.C. Hersam, A.J. Freeman, T.J. Marks, CdO as the archetypical transparent conducting oxide. Systematics of dopant ionic radius and electronic structure effects on charge transport and band structure, J. Amer. Chem. Soc. 127 (2005) 8796–8804.
[11] K.M. Yu, M.A. Mayer, D.T. Speaks, H. He, R. Zhao, L. Hsu, S.S. Mao, E.E. Haller, W. Walukiewicz, Ideal transparent conductors for full spectrum photovoltaics, J. Appl. Phys. 111 (2012) (123505-1-5).
[12] D.M. Detert, S.H.M. Lim, K. Tom, A.V. Luce, A. Anders, O.D. Dubon, K.M. Yu, W. Walukiewicz, Crystal structure and properties of CdxZn1–xO alloys across the full composition range, Appl. Phys. Lett. 102 (2013) 232103.
[13] D.M. Detert, K. Tom, C. Battaglia, J. Denlinger, S.H.M. Lim, A. Javey, A. Anders, O.D. Dubon, K.M. Yu, W. Walukiewicz, Fermi level stabilization and band edge energies in $Cd_xZn_{1-x}O$ alloys, J. Appl. Phys. 115 (2014) 233708.
[14] G. Chen, K.M. Yu, L.A. Reichertz, W. Walukiewicz, Material properties of $Cd_{1-x}Mg_xO$ alloys synthesized by radio frequency sputtering, Appl. Phys. Lett. 103 (2013) 041902.
[15] Y.Z. Zhu, G.D. Chen, H. Ye, Electronic structure and phase stability of MgO, ZnO, CdO, and related ternary alloys, Phys. Rev. B 77 (2008) 245209.
[16] W. Burstein, Anomalous optical absorption limit in InSb, Phys. Rev. 93 (1954) 632–633.
[17] J.F. Geisz, S. Kurtz, M.W. Wanlass, J.S. Ward, A. Duda, D.J. Friedman, J.M. Olson, W.E. McMahon, T.E. Moriarty, J.T. Kiehl, High-efficiency GaInP/GaAs/InGaAs triple-junction solar cells grown inverted with a metamorphic bottom junction, Appl. Phys. Lett. 91 (2007) 023502.